The effect of variable operating parameters for hydrocarbon fuel formation from CO_2 by molten salts electrolysis

Ossama Al-Juboori[a], Farooq Sher[b,*] Abu Hazafa[c], Muhammad Kashif Khan[d], George Z. Chen[a,e,*]

[a] *Department of Chemical and Environmental Engineering, University of Nottingham, University Park, Nottingham NG7 2RD, UK.*

[b] *School of Mechanical, Aerospace and Automotive Engineering, Faculty of Engineering, Environment and Computing, Coventry University, Coventry CV1 5FB, UK*

[c] *Department of Biochemistry, University of Agriculture, Faisalabad, 38000, Pakistan*

[d] *School of Mechanical Engineering, Sungkyunkwan University, 2066, Seobu-Ro, Jangan-Gu Suwon, Gyeong Gi-Do 16419, Republic of Korea*

e Department of Chemical and Environmental Engineering, Faculty of Science and Engineering, University of Nottingham Ningbo China, University Park, Ningbo 315100, China

**Corresponding authors:*

Email addresses: Farooq.Sher@coventry.ac.uk (F. Sher), George.Chen@nottingham.ac.uk (G.Z. Chen).

Abstract

The emission of CO_2 has been increasing day by day by growing world population, which resulted in the atmospheric and environmental destruction. Conventionally different strategies; including nuclear power and geothermal energy have been adopted to convert atmospheric CO_2 to hydrocarbon fuels. However, these methods are very complicated due to large amount of radioactive waste from the reprocessing plant. The present study investigated the effect of various parameters like temperature (200–500 ^oC), applied voltage (1.5–3.0 V), and feed gas (CO_2/H_2O) composition of 1, 9.2, and 15.6 in hydrocarbon fuel formation in molten carbonate (Li_2CO_3-Na_2CO_3-K_2CO_3; 43.5:31.5:25 mol%) and hydroxide (LiOH-NaOH; 27:73 and KOH-NaOH; 50:50 mol%) salts. The GC results reported that CH_4 was the predominant hydrocarbon product with a lower CO_2/H_2O ratio (9.2) at 275 ^oC under 3 V in molten hydroxide (LiOH-NaOH). The results

also showed that by increasing electrolysis temperature from 425 to 500 ^{o}C, the number of carbon atoms in hydrocarbon species rose to 7 (C_7H_{16}) with a production rate of 1.5 μmol/h cm^2 at CO_2/H_2O ratio of 9.2. Moreover, the electrolysis to produce hydrocarbons in molten carbonates was more feasible at 1.5 V than 2 V due to the prospective carbon formation. While in molten hydroxide, the CH_4 production rate (0.80–20.40 μmol/h cm^2) increased by increasing the applied voltage from 2.0–3.0 V despite the reduced current efficiencies (2.30 to 0.05%). The maximum current efficiency (99.5%) was achieved for H_2 as a by-product in molten hydroxide (LiOH-NaOH; 27:73 mol%) at 275 ^{o}C, under 2 V and CO_2/H_2O ratio of 1. Resultantly, the practice of molten salts could be a promising and encouraging technology for further fundamental investigation for hydrocarbon fuel formation due to its fast-electrolytic conversion rate and no utilization of catalyst.

Keywords: Renewable energy; Molten salt electrolysis; Applied voltage; CO_2/H_2O; hydrocarbon fuels; Electrochemical conversion and Carbon dioxide capture.

1 Introduction

With increasing world population and living standards, the consumption of energy sources (fossil fuels) internationally and domestically has been increased that resulted in high levels of CO_2 in the atmosphere and leading to environmental and climate destructions. The higher concentration of CO_2 is not only causing the greenhouse effect but also affecting global warming, melting the polar ice, and increasing atmospheric temperature [1, 2]. Therefore, the strategies should be adopted to reduce and convert CO_2 directly from emission sources or atmosphere into hydrocarbon fuels by utilizing renewable energy sources including hydroelectric, geothermal, solar, and wind [3, 4]. Recently, stationary carbon-free energy sources namely nuclear electric power, that accounts

28.8% of all energy sources in the U.S [4], have been proposed for fuel production but still. However, this method is still very complicated due to large amount of radioactive waste from the reprocessing plants [5].

The above renewable energy sources do not involve CO_2 sequestration through their electricity generation. To tackle CO_2 emissions efficiently, biomass could be a predominant source of energy (biofuel) due to its easy accessibility, high compatibility with the engine, and cost-effectiveness than the conventional energy production techniques (geothermal, solar, and wind) [6, 7]. According to accumulated data, over the past 30 years, biomass is considered a promising CO_2 energy source due to its high energy production ability and could produce more than 1.04 billion tons of energy per year till 2030 [8]. No renewable energy is needed (as claimed) to convert the biomass into the various kinds of biofuels such as biogas and liquid biofuels [9]. However, the production of biofuels could be a comprehensive approach to minimize the utilization of coal and petroleum in halfway by 2030 [8]. The energy efficiency of woody biomass conversion (for instance) to bio-syngas is up to 70–72%. However, the cost of bio-methanol, bio-ammonia and bio-dimethyl ether (DME) produced from syngas derived with forest residues, is still higher than the cost of their fossil fuels-derived counterparts [10, 11].

However, renewable energy resources are often unstable and require an energy storage facility system such as the case for solar panels and wind turbines. CO_2 capture and conversion (CCC) is, therefore, a suitable technology to store renewable energy in the form of hydrocarbon fuels (CH_4, C_2H_4, C_2H_6, C_3H_8, and C_4H_{10}) or C-rich energy carriers [12, 13]. The four carbon-capturing techniques including chemical absorption, physical adsorption, cryogenic fractionation, and

membrane separation have been reported in the literature for capturing CO_2 from flue gas emitting to the atmosphere. The chemical absorption method uses amine solvents for CO_2 capture from flue gas and considered as one of the most applied techniques due to cost-effectiveness, resistance to water and chemicals, and environmental friendly behaviours [14].

Different types of CO_2 conversion methods including aqueous electrolysis, thermochemical cycles, solid oxide electrolysis, proton exchange membrane, and electrolysis via molten salts are reported in the literature [15-17]. Besides to all techniques, the electrolysis is considered as an effected method to dissociate carbon dioxide into hydrocarbon fuels due to its high CO_2 conversion rate and high current efficiency. An electrolytic cell uses electricity to dissociate CO_2 and H_2O. Generally, this dissociation performed in one step like a semi-batch reaction. The low to high-temperature, and aqueous solution electrolysis have been investigated in accumulated data which involved in the dissociation of CO_2 via an aqueous carbonate or bicarbonate electrolyte using copper or some noble metals like platinum as electrode [16, 17]. But aqueous solution electrolysis cannot be considered as a promising technique due to the use of highly expensive membrane and noble metals like platinum as a cathode. However, despite to all techniques, the electrolysis of molten salt is a promising and widely used method in various industrial applications such as co-reduction of CO_2 and H_2O due to their low cost, high current efficiency, higher solubility of CO_2 gas inside the melt, wide potential window, unique characteristics and low melting point in terms of catalyzing various transformation processes besides their electrolytic features [18]. Different types of molten carbonates including K_2CO_3, Na_2CO_3, Li_2CO_3 (25.0:31.5:43.5) were used to catalyze (for instance) CO_2 at 900 ^oC to increase the CO production rate [19, 20].

A study on molten salt proposed that the soluble $NaVO_3$ addition to carbonate molten salt significantly increased the electrochemical conversion of CO_2 to carbon at a high graphitization degree. The study also revealed that the graphitization degree of carbon products was effectively enhanced with only 0.43 value of I_D/I_G [18]. Another, similar study also reported that the carbonate ions can also be added to the molten chloride salt for enhancing CO_2 reduction at lower melting points, which showed a significant influence in CO_2 conversion when just 1 mol% of K_2CO_3 was added to LiCl-KCl molten salt at 500 ^oC [21]. Bronco and his research group [22] reported the formation of higher carbon fuel molecules such as C_3 and C_4 obtained at lower temperatures by using mixed KCl-LiCl molten salts at 550 ^oC. They also revealed that the lower temperature enhances the selectivity of unsaturated products such as C_2H_4 and C_3H_6. Besides, the reduction of CO_2 to carbon was also investigated in KCl-NaCl eutectic mixture at 700 ^oC with or without adding Li_2CO_3 under the pressure of CO_2 gas. Generally, CO_2 reacts with O^{2-} or OH^- ions to produce carbonate ions according to the following reactions (**Eqs. 1-4**). Then carbonate ions can be electro-reduced in turn to form carbon or CO [23].

$$Cl^- + H_2O \rightarrow HCl + OH^- \quad (1)$$

or

$$2Cl^- + H_2O \rightarrow 2HCl + O^{2-} \quad (2)$$

$$2OH^- + CO_2 \rightarrow CO_3^{2-} + H_2O \quad (3)$$

or

$$CO_2 + O^{2-} \rightarrow CO_3^{2-} \quad (4)$$

Despite molten salt types, the variable parameters such as temperature, cell voltage, catalyst, and CO_2/H_2O ratio also have a significant effect on the conversion of CO_2 to CO and hydrogen. Kaplan et al. [24] reported that CO was a dominant product at 900 ^oC or above when CO_2 reduced in the

absence of water. Like temperature, the use of an appropriate applied voltage is very important. Ijije et al. [25] demonstrated the formation of carbon is favoured at potentials more negative than -1.9 V vs. CO_2-O_2 electrode in ternary molten carbonates at 450 ^oC. Furthermore, they also reported that applying cell voltages higher than this limit during electrolysis may consequence in alkali metal deposition (M) and could result in an indirect chemical reduction of carbonate ions. Moreover, different metals including Ta, Nb, Zr, Al, Ti, and Hf are mostly studied as catalysts to promote the reduction of CO_2 to CO due to their stability at elevated temperatures (>800 ^oC) and forming the oxide layer outside metal surface (which is more conductive at higher temperatures than at lower temperatures), and resultantly promote electrolysis [24].

However, the effect of the CO_2/H_2O ratio and different combinations of temperature including 220, 275, 335, 425, and 500 ^oC are not reported in the literature for molten salt chemistry, particularly using electrochemistry. To the best of our knowledge, for the first time, this has been taken into consideration in present research, the effect of CO_2 and H_2O concentrations on electrolysis in molten salts (carbonate, and hydroxide). The present study explained the influence of process variable parameters including temperature (200–500 ^oC), applied voltage (1.5–3.0 V) and CO_2/H_2O ratio (9.2 and 15.6) in the feed gas on the co-electrolysis of CO_2 and H_2O in two different mixtures of molten salts including carbonate, (Li_2CO_3-Na_2CO_3-K_2CO_3; 43.5:31.5:25 mol%) and hydroxide (LiOH-NaOH; 27:73 and KOH-NaOH; 50:50 mol%) salts. Furthermore, the specific hydrocarbon formation is also discussed in each category of molten salts.

2 Material and methods

2.1 Chemicals

Lithium carbonate **(**Li_2CO_3; ≥99.0%**),** sodium carbonate (Na_2CO_3; ≥99.5%), potassium carbonate (K_2CO_3; ≥99.0%**),** lithium hydroxide (LiOH; ≥98% powder), sodium hydroxide (NaOH; ≥98% pellets), and potassium hydroxide (KOH; 90% flakes) were purchased from Sigma-Aldrich, USA. Carbon dioxide (CO_2; 99.99%) and argon (Ar; 99.99%) were procured from Air products. Labovac 10 mineral oil was purchased from Jencons.

2.2 CO_2 absorption

The CO_2 absorption study was carried out through a house built cylindrical retort with a flange type cover using 316-grade stainless steel (17% Ni, 12% Cr, and 2% Mo; Unicorn Metals) to set up experimental reactor. The reactor was composed of two types of high-temperature vessels including CO_2 storage and absorption vessels with same volume (3.5 L). The retort was 130 mm in internal diameter, 7.5, and 800 mm in wall thickness and vertical length respectively. A 2416CG Eurotherm programmable PID 8 segment controller was employed to control the furnace whose maximum working temperature was set at 1100 ^oC with an accuracy of ±1 ^oC. The furnace temperature was increased gradually in the interval of 200 ^oC until achieving the desired temperature. There was a (80–100 ^oC) gap between the furnace temperature and the one inside the resort (molten salt).

The retort was inserted centrally in the furnace. The gap between the retort wall and the bore of furnace was covered with an alumina board (ZIRCAR Ceramics) on the top of the furnace to reduce heat losses. A rubber gasket was used to seal the retort between the lid (flange cover) and the body over water-cooling jacket. The ceramic tubes were sealed through the lid by two

individual filter adapters (Fisher Scientific Ltd.). The ceramic tubes served actually for both holding electrodes and gas product outlets. The cooling water jacket employed to cool the upper part of the retort to ensure safe handling and to avoid the prospect overheating or melting of silicon bungs (and adapters). The CO_2 (99.99% purity) and Ar (99.99% purity) were supplied by Air Products Ltd. in the respective cylinders at room temperature, separated from each other by switching off the valves. Both cylinders were fitted with a 2-stage gas regulator (GIS Leengate). The outlets of these two gas cylinders were set to 0.12 MPa and connected to rotameters (Roxspur Measurement and control) with a flowrate of 20 to 200 mL/min and 5 to 100 mL/min at ambient temperature and pressure (ATP) for CO_2 and Ar respectively.

After leaving flow meters, CO_2 and Ar were mixed and transfer to a Dreschel bottle (absorption vessel) containing 100 mL Millipore grade deionized water, to obtain the desired content of steam (water vapours) in the gas inlet of the reactor. An alumina crucible (Almath) containing about 100 g molten salts (180 mmol/kg Li-Na-K carbonates, or 180 mmol/kg Li-Na hydroxide) were sat on the bottom of the absorption vessel. The temperature and pressure of the absorption vessel were measured by a YCT-727D thermometer (TC Direct; 3 mm diameter and 310-grade stainless steel) and digital pressure indicator with an accuracy of ±0.01 K and ±0.001 Pa, respectively [26]. The insulated thermocouple was put in the molten salt for approximately 1–2 min to obtain an accurate and stable measurement. The following equation (**Eq. 5**) was used to measure the absorption amount of CO_2.

$$nCO_2 = \frac{P_g V_g - P\left(V_g + V_e - V_m\right) + P_v V_m}{RT} \quad (5)$$

Where $n$$CO_2$(mmol) represents the absorption amount of CO_2 at given time t (min), P(kPa) represents the CO_2 pressure at given time t (min), P_g (kPa) is the initial CO_2 pressure in the gas

storage vessel, P_v(kPa) signify the saturated vapour pressure of eutectic salts, V_e(cm^3) and Vg (cm^3) indicate the volume of absorption and storage gas vessel, and Vc (cm^3) and Vm (cm^3) are the volume of the crucible and molten salts, respectively [27].

2.3 Electrochemical measurements

For CO_2 conversion, different combinations of molten salts including a mixture of molten carbonates (Li_2CO_3-Na_2CO_3-K_2CO_3; 43.5:31.5:25 mol%) at 397 ℃, and two mixtures of molten hydroxides (LiOH-NaOH; 27:73 and KOH-NaOH; 50:50 mol%) at 218 and 170 ℃ were pre-melted respectively [27, 28]. The experiments were performed under CO_2 and Ar atmosphere. Two-electrode mode was conducted to produce fuel gas from CO_2 and H_2O electrolysis, by employing Agilent E3633A 20A/10V Auto-Ranging DC Power Supply and a laptop with MS Excel add-in to collect the instrumentation data. The titanium foil (thickness: 1 mm, purity: 99.99%, Good fellow Cambridge Ltd.), and graphite rod (diameter: 5 mm, purity: 99.99%, Advent Research Materials) were used as working electrode (cathode material) in molten carbonate and molten hydroxide to see the selective production of hydrocarbon species.

Similarly, a stainless-steel rod (304 grades; 6 mm diameter, Unicorn Metals) was used in molten carbonate and hydroxide as a counter electrode or anode material [29]. The electrolysis is designed to study the effect of applied voltage, feed gas composition, temperature, and molten salt composition for the production of fuel gases in general and hydrocarbon species particularly. For electrolysis, the applied voltage was maintained at 1.5 V for the molten carbonate mixture to avoid carbon deposition, which is thermodynamically preferred on the cathode at applied cell voltages above 2 V. For molten hydroxide and chloride, the cell voltage was applied at 2 and 3 V

209 respectively. The primary products including hydrogen and carbon monoxide gases were produced
210 from the reduction of H_2O and CO_2 at cathode [29, 30].

211 2.4 Characterization

212 2.4.1 Gas chromatography (GC)

213 Gas chromatography (GC) was used to analyze the gas products generated from electrolysis. In
214 the present study, PerkinElmer Clarus 580 gas chromatography (GC) instrument was used for
215 analyzing hydrogen evolution and general light hydrocarbons ($<C_6$). The hydrogen, CO, and CO_2
216 gas evolution was detected in a GC instrument equipped with TCD detector thermostated at 160
217 ℃, and a Haysep N6 packed column (60–80, 7'×1/8'' sulfinert) with argon as a carrier gas
218 thermostated at 60 ℃. For hydrocarbon analysis, the GC was equipped with an FID detector and
219 RT® Alumina Bond/KCl capillary column (30 m × 0.32 mm i.d., 5 μm) with helium as a carrier
220 gas [31]. A 5 mL gas sample was taken by gas-tight syringe to a tedler 1 L (SKC Ltd.) gas bag,
221 which then injected into the chromatograph. The gas species in the sample were identified and
222 quantified by comparison with two different gas standards, including permanent gas standard and
223 calibration gas standard. The first one is permanent gas standard with composition of H_2 10%, CO_2
224 10% and CO 40% for TCD detector. The second standard calibration gas contains ethane (C_2H_4)
225 0.2%, propylene (C_3H_6) 0.2%, 1-butene (C_4H_8) 0.2%, 1-pentene (C_5H_{10}) 0.2%, methane (CH_4)
226 20%, ethane (C_2H_6) 10%, propane (C_3H_8) 5%, n-butane (C_4H_{10}) 2%, n-pentane (C_5H_{12}) 1% for the
227 FID detector. The remaining composition of both gas standards was balanced with helium gas.

228 2.4.2 Gas chromatography-mass spectrometry (GC-MS)

229 The unknown hydrocarbon species were analyzed by using Agilent 7890B gas chromatograph
230 interfaced with a JEOL AccuTOF GCX mass spectrometer with ionizing energy of 70 eV and a
231 source temperature of 150 °C. The separation was processed on a fused silica capillary column

(30m × 0.25 mm i.d. × 25 µm) with helium as a carrier gas. The method of oven temperature-programmed was employed from 40 ^{o}C (hold for 18 min) to 350 ^{o}C (hold 2 min) at 25 ^{o}C/min. The gas sample compounds were separated by the GC part that eludes at different times using a silica capillary column. The sample gas has exited the GC, and the compounds were bombarded in the MS part by high energy electrons that detach an electron from each molecule and result in positively charged molecular ions (M^+) ($M + e^- \rightarrow M^+ + 2e^-$). Further, an analyzer works to separate the molecular ions by mass-to-charge ratio (m/z) and was detected by an ion detector [32].

3 Results and discussion

The effect of process variables including temperature, applied cell voltage and CO_2/H_2O ratio on co-electrolysis of CO_2 and H_2O gases themselves and the production of hydrocarbons were examined and discussed in the following sections.

3.1 Effect of temperature

The variation of temperature in hydrocarbon formulation as for any chemical reaction in general affects the rate of reaction and equilibrium position of the molecules produced reversibly during hydrocarbon production process. In molten carbonates, for instance, the temperature can be reduced to the lowest point as possible to maintain the salt in a liquid state on one side and for the sake of hydrocarbon formation preferred thermodynamically on the other side [33]. The temperature effect was studied in a molten carbonate (Li_2CO_3-Na_2CO_3-K_2CO_3; 43.5:31.5:25 mol%) and hydroxides (LiOH-NaOH; 27:73 and KOH-NaOH; 50:50 mol%).

3.1.1 Molten carbonate

The selectivity and production rates for various hydrocarbon species including (CH_4, C_2H_4, C_3H_6, C_4H_8, C_6H_{14}, and C_7H_{16}) were investigated in molten carbonates (Li_2CO_3-Na_2CO_3-K_2CO_3;

43.5:31.5:25 mol%) at two different temperatures (425 and 500 ^{o}C) under 1.5 V using a gas feed composition of 48.4% (CO_2) + 3.2% (H_2O) + 48.4% (Ar) in two runs. The surface area of titanium plate cathode was 5.9 cm^2 [34]. The selectivity of the hydrocarbon species was calculated by the proportion of moles of desired hydrocarbon species to the moles of undesired products of H_2 and CO [35]. The FID analysis revealed a slight decrease in H_2 production rate could be attributed to the formation of new hydrocarbon species (C_6H_{14} and particularly C_7H_{16}) as presented in **Fig. 1**. The presence of C_7H_{16} was detected by GC-mass spectrometry analysis as it cannot be confirmed through normal GC. The findings presented in **Table 1** and **Table 2** report the selectivity for different hydrocarbon species. It is confirmed, the selectivity of CH_4, C_3H_6, and C_4H_8 was relatively good at 425 ^{o}C and further enhanced from 7–42% in total at 500 ^{o}C due to lower rates of H_2 and CO formation in the final products.

In addition, the formation of higher molecular weight products (such as C_6H_{14} and C_7H_{16}) with small production rates (2.4 and 1.2 μmol/h cm^2 respectively) offer a calorific heat value (heating value or the heat of combustion) by ten times the amount for H_2 or CO. The findings also revealed that the total energy consumption at 425 ^{o}C under 1.5 V for low molecular weight hydrocarbon products (CH_4, C_3H_6, and C_4H_8) was 114.2 J. While at 500 ^{o}C under same conditions for higher hydrocarbon products (C_6H_{14}, and C_7H_{16}), the energy consumption was 171 J, which indicates that the higher hydrocarbons consume more energy than the lower hydrocarbons due to their greater size and compound complexity. Therefore, based on these findings, it is concluded that the lower temperature is more feasible for hydrocarbon fuel production than higher temperature because the higher temperature consumes more energy than lower. Wu et al. [36] reported the CO_2 reduction into carbon species at 600 ^{o}C in an electrolysis, containing a mixture of carbonate using iron as a

cathode electrode showed the current densities of 50, 100, and 200 mA/cm^2 for carbon materials (C, O, and CO).

Another experiment conducted on binary molten carbonate Li_2CO_3-Na_2CO_3 (52–48 mol%) at 600 ^oC under $P_{CO2=}$1 bar demonstrated that Li_2CO_3 in molten salt lowered the melting point of the mixture which resultantly enhanced the process of carbon deposition, but it requires higher energy for CO_2 reduction [37]. The analysis of the mass spectrum (see **Fig. 2)** confirmed the identification of hydrocarbons higher than C_5 products as clear fragments lost from the last specified hydrocarbon during the analysis (44 for C_3H_8, 56 for C_4H_8, 84 for C_6H_{12}, 98 for C_7H_{14} and 112 for C_8H_{16}). Furthermore, the data suggested that the electrolytic voltage (1.5 to 1.49 V) that is required to convert CO_2 and H_2O to CO and hydrogen gas decreased by increasing temperature (425–500 ^oC). Liu et al. [38] reported that electrolytic voltage decreased from 1.15 to 0.91 V by increasing temperature from 300 to 1000 ^oC for CO_2 and H_2O conversion. They also revealed that hydrocarbon like CH_4 was thermodynamically preferred below 575 ^oC and lower voltage whereas the CO was thermodynamically preferred above 800 ^oC when CO_2 was converted separately. The study also demonstrated that three different reduction peaks at -1.0, -0.5, and 0.0 electrolytic voltage confirmed the formation of H_2, CH_4, and CO, respectively at 600 ^oC in molten carbonate ($Li_{1.48}Na_{0.52}CO_{3.00}$) by using Fe (0.3 cm^2) and Ni (0.3 cm^2) as cathode and anode electrode respectively [38].

3.1.1.1 Theoretical justification of C_7H_{16} formation

For the conventional formation of C_7H_{16} (for instance) by Fischer-Tropsch process, numerous moles of CO and H_2 are involved to formulate final compound [39, 40], the possible reactions are presented as follows (**Eqs. 6-8**):

$$7CO + 15H_2 \rightarrow C_7H_{16} + 7H_2O\,(g)\,\Delta G_{500C} = 154.1\,KJ/mol \quad (6)$$

$$14CO + 8H_2 \rightarrow C_7H_{16} + 7CO_2\,(g)\,\Delta G_{500C} = 81.43\,KJ/mol \quad (7)$$

$$7CH_4 + 3O_2 = C_7H_{16} + 6H_2O\,(g)\,\Delta G_{500C} = -866.6\,KJ/mol \quad (8)$$

The products of hydrocarbons and their ΔG of formation by Fischer-Tropsch reactions (CO_2 or H_2O formation) and by partial oxidation of methane at 500 ºC under 1.5 V are presented in **Table 3**. According to the findings, it is clear that the formulation of C_7H_{16} from the partial oxidation of methane is more feasible as the formation of CH_4 itself at temperatures up to 500 ºC. In general, hydrocarbon formation behaves like carbon deposition in terms of the process variables during CO_2 reduction in molten carbonates. Therefore, process variables affecting carbon product from the CO_2 sole conversion (without H_2O) act as a sequential effect on the hydrocarbon formation after H_2O addition. It has been found that temperature has an important influence on the morphology and particle size of deposited carbon [41]. The particle size of carbon increases with increasing electrolysis temperature (335–520 ℃) and results in carbon deposition that could be denser (although not quicker).

The existence of C_2H_4 (even a low intensity peak) as an olefin beside paraffin (alkane) at high temperatures (as shown in **Fig. 1(a)**) justified the formation of long chain hydrocarbons like C_6H_{14} or C_7H_{16} through the following reactions (**Eqs. 9-12**) [40, 42]. Thus, the paraffin like propane was normally alkylated at high temperatures even in the absence of catalyst according to the below mentioned equations due to composed free radicals such as isopropyl radicals **(Eq. 10).** The reaction of isopropyl radical with an olefin **(Eq. 11)** and paraffin **(Eq. 12)** molecule produced higher alkylated products such as C_5H_{12} or alternately, even long chain hydrocarbon molecules.

The polymerization of olefins to high molecular weight hydrocarbons occurred if olefin content in the product has increased.

$$CH_3 - CH_2 - CH_3 \rightarrow C\dot{H}_3 + C_2\dot{H}_5 \quad (9)$$

$$C\dot{H}_3 + CH_3 - CH_2 - CH_3 \rightarrow CH_3 - C\dot{H} - CH_3 + CH_4 \quad (10)$$

$$CH_3 - C\dot{H} - CH_3 + CH_4 \rightarrow CH_3 - CH(CH_3) - CH_3 - C\dot{H}_2 \quad (11)$$

$$CH_3 - CH(CH_3) - CH_3 - C\dot{H}_2 + CH_3 - CH_2 - CH_3 \rightarrow CH_3 - CH(CH_3) - CH_3 - CH_3 + CH_3 - C\dot{H} - CH_3 \quad (12)$$

Indeed, the methyl radical ($CH_3^{\bullet}$) also formed by the partial oxidation of methane in molten carbonates as a perfect medium for oxide ion transformation [43]. The methyl radical then continues to attack other kinds of paraffin like C_3H_8 and produces long straight-chain hydrocarbons or even branched hydrocarbons. It is worthwhile to mention that the methyl radical or any other alkyl radical plays a major role in the formulation of long chain hydrocarbon species from paraffins during thermal alkylation process, even in the absence of a catalyst at a high temperature of 500 ^{o}C. The proportion of CO_2 to H_2O mole ratio affected the formation of large molecular weight species of hydrocarbons (C_5H_{12} or above) [44]. Overall, it is noticed that performing electrolysis at higher temperatures (> 500 ^{o}C) could not lead to the formation of hydrocarbons due to lack of CH_4 formation in general.

3.1.2 Molten hydroxide

The gas product specification results were found to be better in molten carbonate at low temperatures as 425 ^{o}C. The electrolytic temperature in the molten hydroxide (LiOH-NaOH; 27:73

and KOH-NaOH; 50:50 mol%) was increased to investigate the improvement of fuel production and to avoid a rapid carbonate ion formation that formed through **Eq. (3)**.

Fig. 3 illustrates the effect of temperature on the production rates of H_2, CO, and CH_4 during electrolysis of LiOH-NaOH molten salt at 2.0 V cell voltage using a gas feed composition of 48.4% (CO_2) + 3.2% (H_2O) + 48.4% (Ar). KOH-NaOH salt was used in the case of 220 ^oC temperature run because its melting point at 187 ^oC is lower than that of LiOH-NaOH eutectic mixture. Further, **Fig. 3(b)** reported that the H_2 production rate was slightly increased from 164.7 to 185.7 μmol/h cm^2 when the electrolysis temperature was increased from 220 to 275 ^oC respectively at the same applied voltage and then dropped significantly at a lower level of about 41.6 μmol/h cm^2 at 335 ^oC (Fig. 3(c)). However, the production rates for CO and CH_4 were kept at same levels as 0.00 and 6.12 μmol/h cm^2 when the temperature increased from 220 ^oC to 275 ^oC in molten KOH-NaOH (50:50 mol%) and LiOH-NaOH (27:73 mol%) salts respectively. Then inclined gradually to 0.8 μmol/h cm^2 for both CO and CH_4 at 335 ^oC in molten hydroxide (LiOH-NaOH 27:73 mol%).

It has been suggested that by increasing the electrolytic temperature does not significantly improve hydrocarbon production in molten hydroxides (KOH-NaOH 50:50 mol%, and LiOH-NaOH 27:73 mol%). Nevertheless, alkali metal deposition has been predominant at electrolytic temperatures higher than 275 ^oC and at a lower H_2O content in the salt. Possibly consuming higher energy and reducing current efficiencies (15.60 to 0.00%), while H_2O reduction was diminished by this stage as presented in **Fig. 3.**

It also clarified that the values of current efficiencies started as 15.6 and 2.3% for H_2 and CH_4 respectively at 220 ^oC (see **Fig. 3 (a)**) and then slightly decreased as 13.0 and 2.0% respectively at 275 ^oC (see **Fig. 3(b)**), and further to a larger extent as 1.60 and 0.13% respectively at 335 ^oC (see **Fig. 3(c)**) because of alkali metal deposition. It is noticed that hydrocarbon fuel such as methane production rate (6.12 µmol/h cm^2) was significantly higher at 220 ^oC under 2 V in KOH-NaOH (50-50 mol%) molten hydroxide than other two molten hydroxides. Whereas H_2 production rate of (about 185.70 µmol/h cm^2) was maximum at 275 ^oC in molten hydroxide (LiOH-NaOH; 27–73 mol%) under 2 V.

3.2 Applied cell voltage

The molten salts used in the present study showed high thermal and electrochemical stability when various cell voltages were applied particularly at adjusted gas feed composition before the event of alkali metal deposition on cathode. The cell voltage is considered a key variable, it does not only affects the energy consumption or current efficiency but also improves the product properties at the same time [41].

3.2.1 Molten carbonate

The effect of applied cell voltage on carbon deposition in molten carbonates has been confirmed in the literature. Employing higher cell voltages from 4 to 6 V, significantly improved the particle size of deposited carbon but not always increase deposition rate itself [45]. Even, a rapid carbon deposition in the molten carbonates was not preferred for the sake of hydrocarbon formation. Therefore, the cell voltage used for this salt was kept as low as 1.5 V to avoid carbon and alkaline metal deposition that could otherwise commence at 2 V. It was found that the cell voltage of 1.5 V in the molten carbonates is more sufficient to carry out electrolysis [46] for CO_2 and H_2O

individually to produce CO and H_2, before the feasible formation of CH_4 or hydrocarbons in general.

To show the effect of 2 V cell voltage, **Fig. 4** illustrates a significant difference between the average currents at 1.5 and 2 V. While both runs were performed at 500 ^oC with the same gas feed composition, the hydrocarbon formation at 2 V was rare. However, some of the hydrocarbon species (such as CH_4, C_2H_4, and C_5H_{10}) found in the FID results of the previous experiments (425 or 500 ^oC runs at 1.5 V) were still slightly appeared in the FID result of 2 V run at 500 ^oC atleast with quite low contents and production rates (see **Fig. 5**). It is worthwhile to say that hydrocarbons CO and H_2 could be formed on cathode at high temperatures under a cell voltage of 1.5 V, although carbon deposition was not quick enough on cathode [41] to feasibly generate the above hydrocarbon species.

3.2.2 Molten hydroxide

The situation was quite different for the molten hydroxide because the applied cell voltage was increased from 2 to 3 V. By raising the applied cell voltage in LiOH-NaOH salt electrolysis from 2 to 3 V, the production rates of CH_4 increased dramatically by 200% as observed in **Fig. 6** and **Fig.** 7 for 3 V cell applied voltage. This rise in CH_4 production rates as well as the generation of CO in the second run of 3 V counted as further evidence for CO_2 reduction in molten hydroxides as the production rate of H_2 decreases by half of the value obtained in the 2 V run. The mitigation of H_2 rate suggests a rapid formation of CO and CH_4 from CO_2 reduction with a possible electro-deposition of alkali metal at high cell voltage, which consequently affected the current efficiencies of the products.

The predominant formation of CH_4 rather than other kind of hydrocarbons (C_3H_6, C_4H_{10}, C_5H_{12}, and C_6H_{14}) was because of the lack of partial oxidation in molten hydroxide in contrast with molten carbonates mediums. Ji et al. [47] revealed that the electrolytic reduction of C_4^+ from carbonates leads to the formation of H^+ in molten hydroxide. By comparing the potassium, lithium, and sodium atoms, the lithium atom has a shorter radius and strong binding among all, which indicated that the lithium hydroxides have greater deposition voltage. Due to this admirable advantage, the lithium hydroxide gives relatively stable H^+ with minimum energy losses and reactions. As previously stated, that peroxide ions (O_2^{2-}) are largely responsible for the partial oxidation in molten salts [48]. The formation of this type of reactive oxides, unfortunately, was quite absent in the molten hydroxide due to the acidic nature of the salt, even in the presence of minor amounts of H_2O.

3.3 CO_2/H_2O ratio

The CO_2/H_2O ratio is one of the most important variables in the electrolysis. It has been considered due to the prospective effect of CO_2 and H_2O reduction before the complete formation of hydrocarbons. Generally, the more H_2O content in the feed gas (or less CO_2/H_2O ratio), the more is H_2 content in the cathodic gas product with a subsequent reduction in the output of hydrocarbon species [49]. However, it is necessary to keep CO_2 concentration in the gas feed composition of 48.4% (CO_2) + 3.2% (H_2O) + 48.4% (Ar) at moderate levels in some of the molten salts including molten carbonates and hydroxides even for the sake of H_2 production.

3.3.1 Molten carbonate

In this experiment, two runs were performed with two different gas feed compositions as CO_2/H_2O=9.2 and CO_2/H_2O=15.6 at 425 ^oC. Furthermore, two more runs were performed with same the gas feed composition at 500 ^oC under 1.5 V for both cases. The findings of CO_2/H_2O=9.2

run at 425 °C showed that the H_2 production rate (95.05 µmol/h cm^2) was more than twenty times the rate obtained at CO_2/H_2O=15.6 (4.40 µmol/h cm^2), these results are presented in **Fig. 8**. Indeed, H_2O vapour content in the gas feed was not enlarged in the second run but the CO_2 content itself was reduced instead by diluting the feed gas with Ar. However, hydrocarbon fuel formation rather than CH_4, in general, was rare in the second run obviously because of the high rate of H_2O reduction to H_2 and lower feasibility of hydrocarbon formation. However, CH_4 was the predominant hydrocarbon fuel, though in this case.

In the case of the 500 °C run, it was noticed that an increase in H_2O content in the gas feed does not lead to higher H_2 production rates as for 425 °C (from fast or rapid H_2O reduction). H_2 production rates were not increased at higher levels possibly because of lower H_2O solubility, and reduction of HCO_3^- ions that were produced from H_2O conversion to H_2 (see **Fig. 9).** The presence of CO_2 at an adequate content in the feed gas was important with H_2O vapour to produce H_2 in addition to CO and hydrocarbons at 1.5 V. Moreover, it was recorded that the solubility of CO_2 increased in the molten carbonates by increasing the temperature through which H_2O solubility was decreased in turn.

The partial oxidation of methane, therefore, can occur even at CO_2/H_2O ratio of 9.2. The CH_4 was confirmed from the first peek at approximately 2 min retention time during FID analysis from GC **Fig. 10(a-c).** For C_2H_4, the peak was confirmed at around 3 min for the same analysis from gas samples of the standard mixture. The peak with m/z value of 28 in the mass spectrum (see **Fig. 11**) could be proved for CO or C_2H_4. However, peak with m/z value of 14 is shown as a tiny peak in the loss of fragrant CH_2 from C_2H_4 molecules and another small peak of 32 m/z is for the O_2. Peaks

with m/z values of 18, 40 and 44 subsequently stand for H_2O, Ar and CO_2 molecules respectively. White and Twardoch, [50] suggested that in the case of carbonate molten salts, changing water composition in the feed gas mixture of CO_2-H_2O at a relatively low CO_2 concentration (<25% volume of feed gas) plays a major role in H_2 gas evolution. They also studied that H_2 evolution peaks were found more clearly by high current density on cyclic volumetric performed at the lowest value of CO_2 partial pressure of 7.4 mm Hg. However, there was no evidence actually about the effect of water composition at higher CO_2 concentrations (>75% volume of feed gas).

By comparing **Fig. 12(a)** for the mass spectrum of gas molecule (C_7H_{10} or more) eluting at 1.72 min retention time with **Fig. 12(b)** for the spectrum of C_8H_{18} standard elution at approximately 2.9 min in a different analysis at the same temperature-programmed (method), it can be seen that the gas follows the same behaviour as the standard and can be identified as C_7H_{16}. There is no prominent peak of an even number to show the spectrum of the total ion resulting from the hydrocarbon molecule except 100 (for C_7H_{16}) as the peak was clarified for C_8H_{18} as 114 in **Fig. 12(b)**, thus holding a lower intensity than its fragments (72 for C_5H_{12}, 58 for C_4H_{10}, and 44 for C_3H_8). The adjacent fragments from C_8H_{18} (99 for C_7H_{15}) and C_7H_{16} (85 for C_6H_{13}) were not shown in both figures because of the loss of peak 29 (CH_3CH_2) already from both molecules.

The formation of higher hydrocarbon species (over C_6H_{14}) justified due to dense carbon deposition or high CO adsorption at cathode because of the high partial pressure of CO_2, particularly in the case of CO_2/H_2O=15.6 as confirmed in the investigations of dry CO_2 reduction [45]. Also, the reduction of CO_2 to CO or C can occur at less reductive potentials than the case for lower partial pressures of CO_2 in the feed gas [51]. Chery et al. [52] stated that the cathodic peaks were increased

with CO_2 partial pressure in both cases (of high and low CO_2 concentrations) as the current density increases with increasing CO_2 partial pressure. In other words, the rise in P_{CO2} increases the amount of dissolved CO_2 in the melt and consequently the amount of CO formed by CO_2 reduction.

3.3.2 Molten hydroxide

Despite the high reactivity of CO_2 with molten hydroxide, this gas (CO_2) itself could be reduced directly during electrolysis to produce CO or hydrocarbon fuels. The presence of large amount of H_2O in the feed gas composition can be a solution to avoid carbonate ion formation by driving **Eq. (13)** in the opposite direction. However, the introduction of a higher content of H_2O in the gas feed due to CO_2/H_2O ratio of 1, was unfortunately led to higher H_2 content than hydrocarbons or CO in the cathodic gas product. Therefore, the employment of moderate H_2O compositions in the feed gas such as a CO_2/H_2O of 5.6 in the electrolysis of LiOH-NaOH (27–73% Mol) at 2 V and 275 °C, led to the production of cathodic gas product with less H_2 (0.91 µmol/h cm^2) and higher CH_4 (6.30 µmol/h cm^2) as shown in

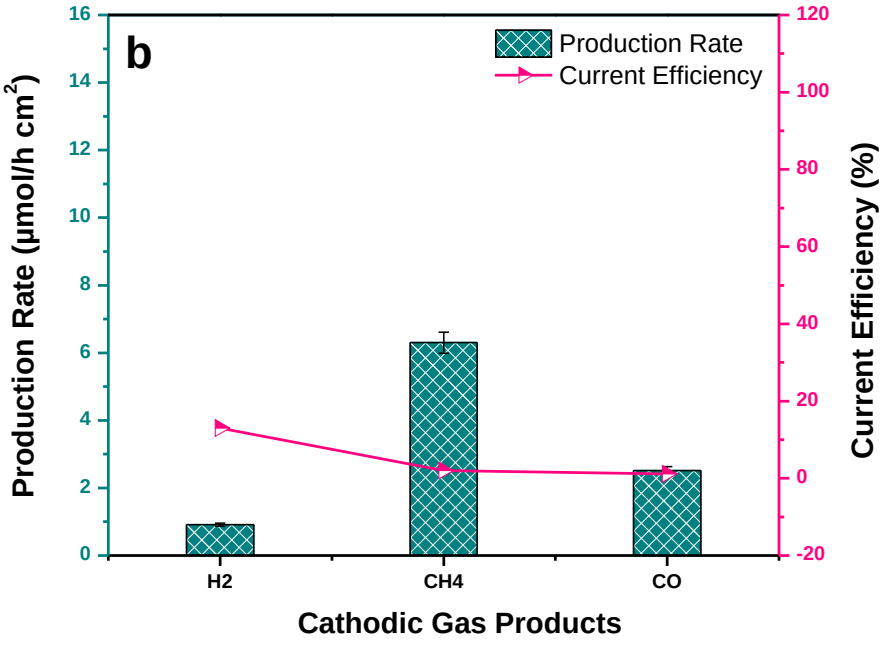

Fig. *13*.

Although carbonate ions formed in both cases, following points were observed about the gas product: (1) The CO was produced exclusively in the second run as it was absent in the first run. This confirms the effect of CO_2 content on electrolysis in the molten hydroxide despite a rapid reaction of CO_2 with the salt, (2) The H_2 production rate was reduced by 16% compared to the first run and (3) The CH_4 production rate was increased more than six times to the rate obtained during the first run. It was also observed that retaining water vapor in the feed gas composition by the above CO_2/H_2O ratio of 5.6 was important to achieve reasonable amounts of H_2, CO, and hydrocarbons during electrolysis. Therefore, performing electrolysis at moderate CO_2/H_2O ratios between 5 and 6 could contribute to achieve reasonable production rates of CH_4, at least with lower H_2 and CO production rates. Liu et al. [53] reported that the co-electrolysis of CO_2/H_2O in molten salts can be used to produce hydrocarbon fuels by Fischer-Tropsch reactions to convert electrical energy to chemical energy. Liu et al. [38] demonstrated that the co-electrolysis of CO_2/H_2O ratio of about 1.96–7.97 in lithium hydroxide at 600 ℃ and current efficiency of 92% significantly lead to one-pot formation of syngas.

4 Conclusions

In summary, the formation of hydrocarbon fuels including; CH_4, C_2H_4, C_4H_8, and C_7H_{16} were achieved through a rationally designed molten salt electrolysis system. In the present examination, the electrolysis was carried out at different temperatures (220–500 ℃), applied cell voltages (1.5, 2, and 3 V) and CO_2/H_2O ratios (15.6, 9.2, and 5.6) in molten carbonate (Li_2CO_3-Na_2CO_3-K_2CO_3; 43.5:31.5:25 mol%) and hydroxides (LiOH-NaOH; 27:73 and KOH-NaOH; 50:50 mol%) to investigate the improvements in fuel production by using cost-effective Ti cathode and Ni anode.

MS analysis confirmed the formation of various new hydrocarbon species (CH_4, C_2H_4, C_4H_8, C_6H_{14}, and C_7H_{16}) with molecules higher than C_5 in molten carbonate by electrolysis at a higher temperature of 500 ^oC and electric voltage of 1.5 V due to the persistent reduction of H_2O to H_2. Besides, this behavior regarding H_2 production rates was found even in the molten hydroxide when the electrolytic temperature was increased from 220 to 275 ^oC with unchanged flow rates of CO and CH_4. The production rates as 41.6, 0.8, and 0.8 μmol/h cm^2 and current efficiencies as 1.6, 0.13, and 0.03% for H_2, CO and CH_4 respectively, declined though to very low values at a higher electrolysis temperature of 335 ^oC in molten hydroxide. Moreover, by applied cell voltage effects, it was confirmed that electrolysis and hydrocarbon formation in molten carbonates were more feasible at 1.5 V than the case of 2 V due to prospective carbon formation. Even with the molten hydroxide, CH_4 production rates (6.12–20.40 μmol/h cm^2) were increased dramatically when the applied voltage was improved from 2 to 3 V despite the reduced current efficiencies. The GC results for the effect of CO_2/H_2O ratio of inlet gas reported that CH_4 was the predominant hydrocarbon product with a high production rate of H_2 formation at lower CO_2/H_2O ratios (9.2) at 500 ^oC in molten carbonates under 1.5 V. However, despite the low production rates, some hydrocarbon products with higher molecular weights (C_6H_{14}, and C_7H_{16}) were also generated when electrolysis was carried out at higher ratios of CO_2/H_2O (15.6) in the feed gas at 500 ℃. Overall, the CH_4 gas was the predominant hydrocarbon fuel produced during the whole electrolysis in pure molten salts under mixed CO_2 and steam in general, and particularly at 275 ^oC. However, it is recommended for future work to analyze anodic gas product beside the cathodic one (by GC) to know the accurate amounts of the entire products from electrolysis in addition to the un-reacted CO_2. Further, a study of process variables including temperature, applied voltage and CO_2/H_2O

ratio in the inlet gas should be performed for molten chlorides beside the molten carbonates and hydroxides for better results.

Acknowledgments

The authors are grateful for the financial supports from the EPSRC (EP/J000582/1 and EP/F026412/1), and Ningbo Municipal People's Government (3315 Plan and 2014A35001-1).

References

1. Hansen, S., A. Mirkouei, and L.A. Diaz, A comprehensive state-of-technology review for upgrading bio-oil to renewable or blended hydrocarbon fuels. Renewable Sustainable Energy Reviews, 2020. 118: p. 109548.
2. Esteves, A.F., et al., The Effect of Light Wavelength on CO2 Capture, Biomass Production and Nutrient Uptake by Green Microalgae: A Step Forward on Process Integration and Optimisation. Energies, 2020. 13(2): p. 333.
3. Kablar, N.A., Renewable Energy: Wind Turbines, Solar Cells, Small Hydroelectric Plants, Biomass, and Geothermal Sources of Energy. Journal of Energy Power Engineering, 2019. 13: p. 162-172.
4. Zheng, Y., et al., A review of high temperature co-electrolysis of H 2 O and CO 2 to produce sustainable fuels using solid oxide electrolysis cells (SOECs): advanced materials and technology. Chemical Society Reviews, 2017. 46(5): p. 1427-1463.
5. Prăvălie, R. and G. Bandoc, Nuclear energy: Between global electricity demand, worldwide decarbonisation imperativeness, and planetary environmental implications. Journal of environmental management, 2018. 209: p. 81-92.
6. Zhao, B., Why will dominant alternative transportation fuels be liquid fuels, not electricity or hydrogen? Energy Policy, 2017. 108: p. 712-714.
7. Hassan, M.H.A., et al., Kinetic and thermodynamic evaluation of effective combined promoters for CO2 hydrate formation. Journal of Natural Gas Science and Engineering, 2020: p. 103313.
8. Kanaujia, P.K., et al., Review of analytical strategies in the production and upgrading of bio-oils derived from lignocellulosic biomass. Journal of Analytical Applied Pyrolysis, 2014. 105: p. 55-74.
9. Karatzos, S., et al., Drop-in biofuel production via conventional (lipid/fatty acid) and advanced (biomass) routes. Part I. Biofuels, Bioproducts Biorefining, 2017. 11(2): p. 344-362.
10. Seiler, J.-M., et al., Technical and economical evaluation of enhanced biomass to liquid fuel processes. Energy, 2010. 35(9): p. 3587-3592.
11. Sher, F., et al., Thermal and kinetic analysis of diverse biomass fuels under different reaction environment: A way forward to renewable energy sources. Energy Conversion and Management, 2020. 203: p. 112266.
12. Budzianowski, W.M., Negative carbon intensity of renewable energy technologies involving biomass or carbon dioxide as inputs. Renewable and Sustainable Energy Reviews, 2012b. 16(9): p. 6507-6521.
13. Al-Shara, N.K., et al., Electrochemical investigation of novel reference electrode Ni/Ni (OH) 2 in comparison with silver and platinum inert quasi-reference electrodes for electrolysis in eutectic molten hydroxide. International Journal of Hydrogen Energy, 2019.
14. Ahmed, R., et al., Recent advances in carbon-based renewable adsorbent for selective carbon dioxide capture and separation-A review. Journal of Cleaner Production, 2019: p. 118409.
15. Redissi, Y. and C. Bouallou, Valorization of Carbon Dioxide by Co-Electrolysis of CO2/H2O at High Temperature for Syngas Production. Energy Procedia, 2013. 37(0): p. 6667-6678.

16. Graves, C., et al., Sustainable hydrocarbon fuels by recycling CO2 and H2O with renewable or nuclear energy. Renewable and Sustainable Energy Reviews, 2011. 15(1): p. 1-23.
17. Carmo, M., et al., A comprehensive review on PEM water electrolysis. International Journal of Hydrogen Energy, 2013. 38(12): p. 4901-4934.
18. Chen, Y., et al., Electrochemical graphitization conversion of CO2 through soluble NaVO3 homogeneous catalyst in carbonate molten salt. Electrochimica Acta, 2020. 331: p. 135461.
19. Wang, P., et al., Corrosion behaviour and mechanism of nickel anode in SO42-containing molten Li2CO3-Na2CO3-K2CO3. Corrosion Science, 2020: p. 108450.
20. Al-Shara, N.K., et al., Electrochemical study of different membrane materials for the fabrication of stable, reproducible and reusable reference electrode. Journal of Energy Chemistry, 2020.
21. Song, Q., et al., Electrochemical deposition of carbon films on titanium in molten LiCl–KCl–K2CO3. Thin Solid Films, 2012. 520(23): p. 6856-6863.
22. Branco, J.B., et al., Catalytic oxidation of methane on KCl-MClx (M = Li, Mg, Co, Cu, Zn) eutectic molten salts. Journal of Molecular Liquids, 2012. 171: p. 1-5.
23. Kamali, A.R. and D.J. Fray, Large-scale preparation of graphene by high temperature insertion of hydrogen into graphite. Nanoscale, 2015. 7(26): p. 11310-11320.
24. Kaplan, V., et al., Conversion of CO2 to CO by Electrolysis of Molten Lithium Carbonate. Journal of The Electrochemical Society, 2010. 157(4): p. B552-B556.
25. Ijije, H.V., R.C. Lawrence, and G.Z. Chen, Carbon electrodeposition in molten salts: electrode reactions and applications. RSC Advances, 2014. 4(67): p. 35808-35817.
26. Ijije, H.V., Electrochemical conversion of carbon dioxide to carbon in molten carbonate salts. 2015, University of Nottingham: Cenrtal Store.
27. Deng, B., et al., Molten salt CO2 capture and electro-transformation (MSCC-ET) into capacitive carbon at medium temperature: effect of the electrolyte composition. Faraday discussions, 2016. 190: p. 241-258.
28. Ji, D., et al., The optimization of electrolyte composition for CH4 and H2 generation via CO2/H2O co-electrolysis in eutectic molten salts. International Journal of Hydrogen Energy, 2019. 44(11): p. 5082-5089.
29. Chen, X., et al., Tuning the preferentially electrochemical growth of carbon at the "gaseous CO2-liquid molten salt-solid electrode" three-phase interline. Electrochimica Acta, 2019. 324: p. 134852.
30. Xu, Y., et al., Direct preparation of V-Al alloy by molten salt electrolysis of soluble NaVO3 on a liquid Al cathode. Journal of Alloys Compounds, 2019. 779: p. 22-29.
31. Huan, T.N., et al., Cu/Cu2O electrodes and CO2 reduction to formic acid: Effects of organic additives on surface morphology and activity. Chemistry–A European Journal, 2016. 22(39): p. 14029-14035.
32. Christian, G.D., P.K. Dasgupta, and K. Schug, Analytical chemistry. 2014.
33. Carrillo, A.J., et al., Solar energy on demand: A review on high temperature thermochemical heat storage systems and materials. Chemical reviews, 2019. 119(7): p. 4777-4816.
34. Du, K., et al., Durability of platinum coating anode in molten carbonate electrolysis cell. Corrosion Science, 2019. 153: p. 12-18.
35. Al Hunaidy, A.S. and S. Souentie, Method and system for capturing high-purity co2 in a hydrocarbon facility. 2019, Google Patents.

36. Wu, H., et al., Effect of molten carbonate composition on the generation of carbon material. RSC advances, 2017. 7(14): p. 8467-8473.
37. Chery, D., et al., Thermodynamic and experimental approach of electrochemical reduction of CO2 in molten carbonates. International Journal of Hydrogen Energy, 2014. 39(23): p. 12330-12339.
38. Liu, Y., et al., Effect of CaCO3 addition on the electrochemical generation of syngas from CO2/H2O in molten salts. International Journal of Hydrogen Energy, 2017. 42(29): p. 18165-18173.
39. Kulikova, M.V., The new Fischer-Tropsch process over ultrafine catalysts. Catalysis Today, 2019.
40. Yang, J., et al., Fischer–Tropsch Synthesis: Using Deuterium as a Tool to Investigate Primary Product Distribution. Catalysis letters, 2014. 144(3): p. 524-530.
41. Tang, D., et al., Effects of applied voltage and temperature on the electrochemical production of carbon powders from CO2 in molten salt with an inert anode. Electrochimica Acta, 2013. 114: p. 567-573.
42. Shafer, W.D., et al., Fischer–Tropsch: Product Selectivity–The Fingerprint of Synthetic Fuels. Catalysts, 2019. 9(3): p. 259.
43. Nourbakhsh, H., et al., Experimental and numerical study of syngas production during premixed and ultra-rich partial oxidation of methane in a porous reactor. International Journal of Hydrogen Energy, 2019. 44(60): p. 31757-31771.
44. Akhmedov, V. and A. Ismailzadeh, The Role of CO 2 and H 2 O in the Formation of Gas-Oil Hydrocarbons: Current Performance and Outlook. Journal of Mathematics, 2019. 6(10).
45. Ijije, H.V., C. Sun, and G.Z. Chen, Indirect electrochemical reduction of carbon dioxide to carbon nanopowders in molten alkali carbonates: Process variables and product properties. Carbon, 2014. 73: p. 163-174.
46. Yin, H., et al., Capture and electrochemical conversion of CO2 to value-added carbon and oxygen by molten salt electrolysis. Energy & Environmental Science, 2013. 6(5): p. 1538-1545.
47. Ji, D., et al., A comparative study of electrodes in the direct synthesis of CH4 from CO2 and H2O in molten salts. International Journal of Hydrogen Energy, 2017. 42(29): p. 18156-18164.
48. Sarvghad, M., T. Chenu, and G. Will, Comparative interaction of cold-worked versus annealed inconel 601 with molten carbonate salt at 450 C. Corrosion Science, 2017. 116: p. 88-97.
49. Kopyscinski, J., C.A. Mims, and J.M. Hill, Formation of CH4 during K2CO3-catalyzed steam gasification of ash-free coal: Influence of catalyst loading, H2O/H2 ratio, and heating protocol. Energy Fuels, 2015. 29(11): p. 6970-6977.
50. White, S.H. and U.M. Twardoch, The electrochemical behaviour of solutions of molten ternary alkali carbonate mixture equilibrated with carbon dioxide-water mixtures at 460°C. Electrochimica Acta, 1984. 29(3): p. 349-359.
51. Chery, D., V. Lair, and M. Cassir, CO2 electrochemical reduction into CO or C in molten carbonates: a thermodynamic point of view. Electrochimica Acta, 2015. 160: p. 74-81.
52. Chery, D., et al., Mechanistic approach of the electrochemical reduction of CO2 into CO at a gold electrode in molten carbonates by cyclic voltammetry. International Journal of Hydrogen Energy, 2016. 41(41): p. 18706-18712.

53. Liu, Y., et al., Syngas production: diverse H 2/CO range by regulating carbonates electrolyte composition from CO 2/H 2 O via co-electrolysis in eutectic molten salts. RSC advances, 2017. 7(83): p. 52414-52422.

List of Figures

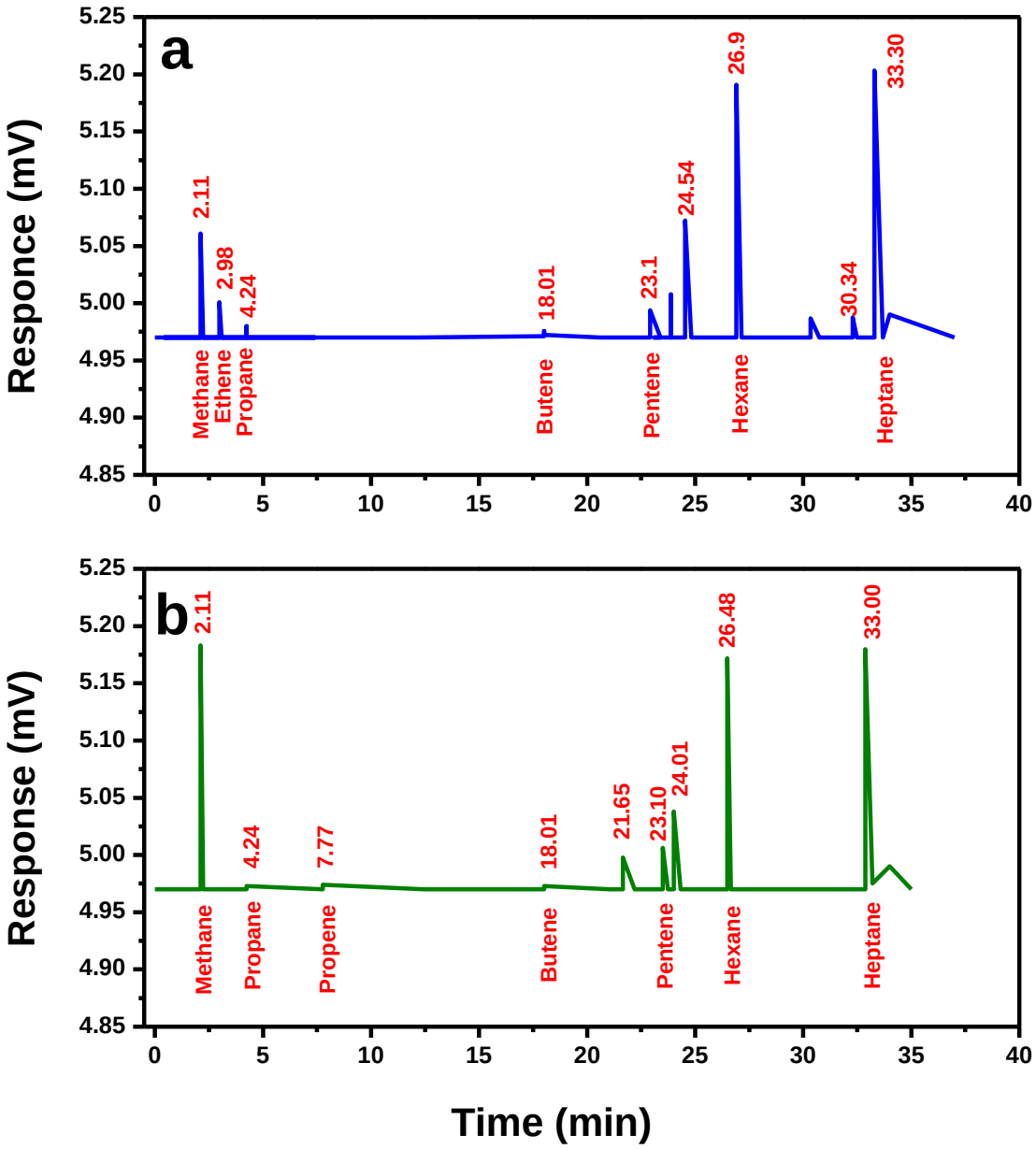

Fig. 1. FID detector analysis of cathodic gas sample taken during the electrolysis of molten carbonates at 1.5 V and 500 ℃ with different CO_2/H_2O ratios; (a) 15.6 and (b) 9.2.

693
694

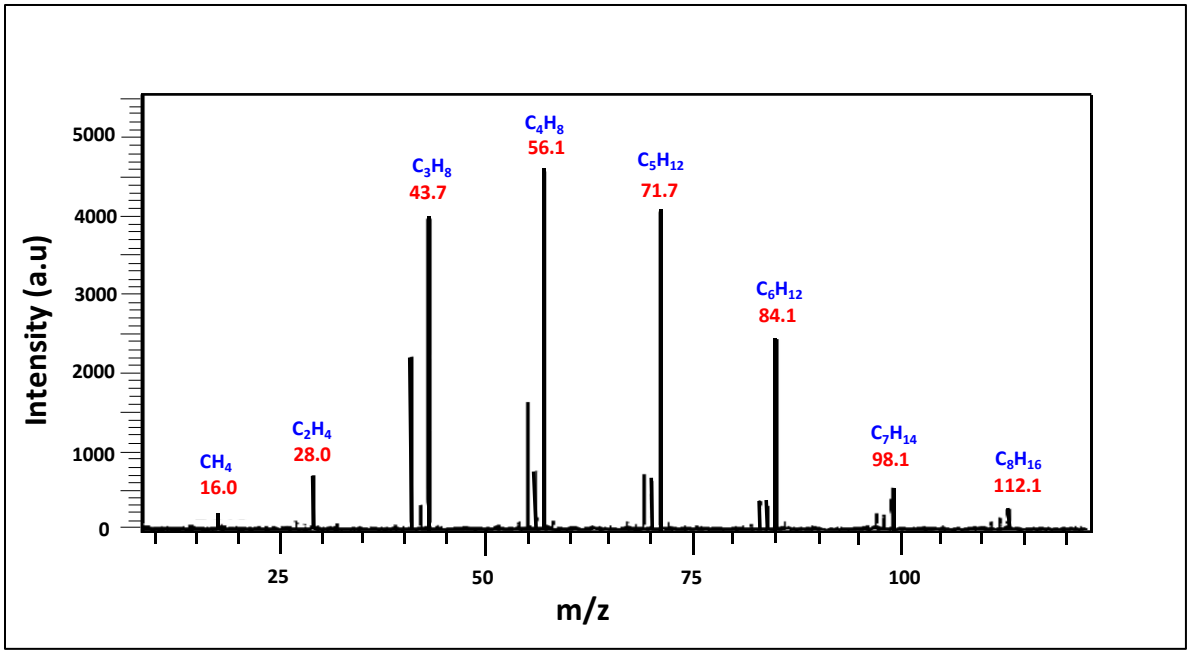

695

696 **Fig. 2.** The mass spectrum of compounds eluting at 18 min retention time in MS-GC analysis
697 during electrolysis of molten carbonates under 1.5 V at 500 ℃ with gas feed composition of
698 CO_2/H_2O=15.6.
699

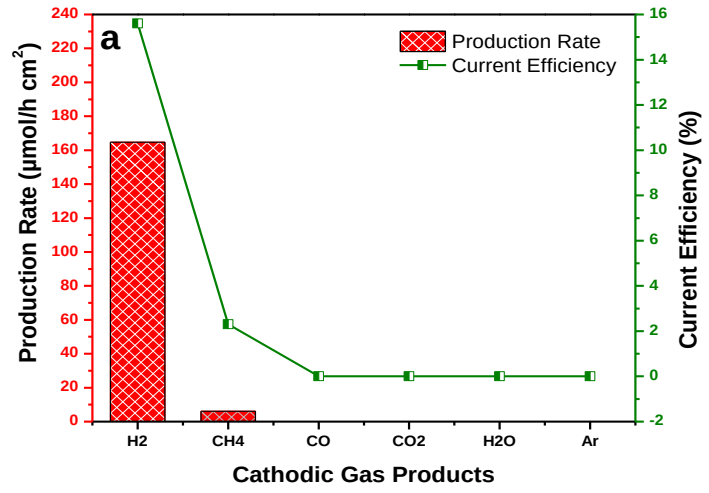

700

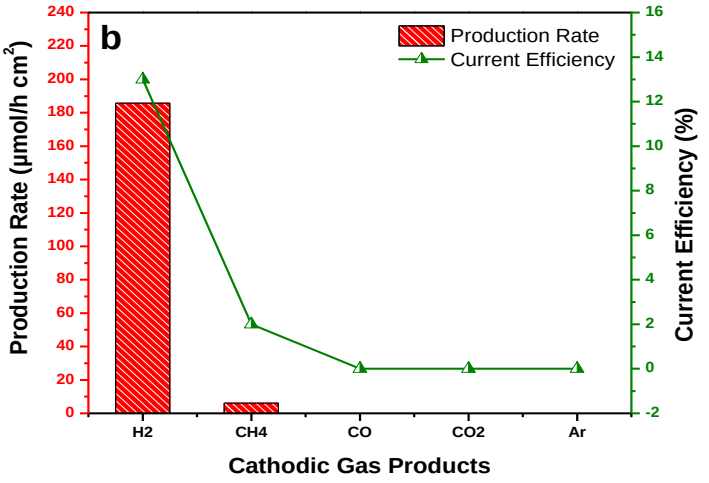

701

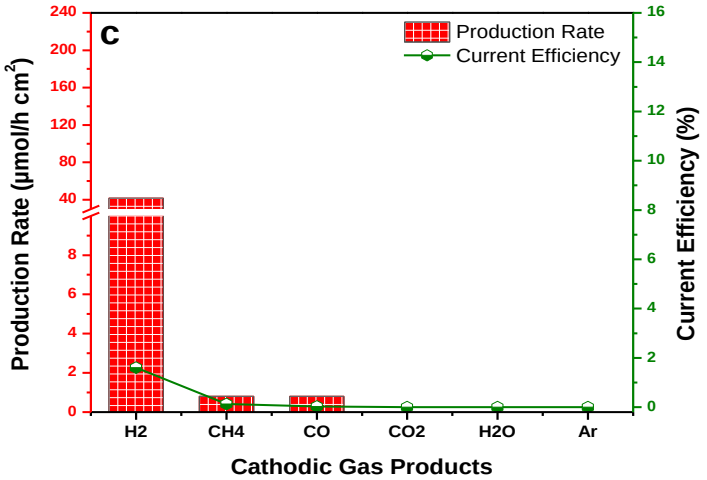

702

703 **Fig. 3**. The cathodic gas products during the electrolysis in molten hydroxide; (a) KOH-NaOH
704 (50–50 mol%) at 220 ℃ (b) LiOH-NaOH (27–73 mol%) at 275 ℃, and (c) LiOH-NaOH (27–73
705 mol%) at 335℃ under 2 V.

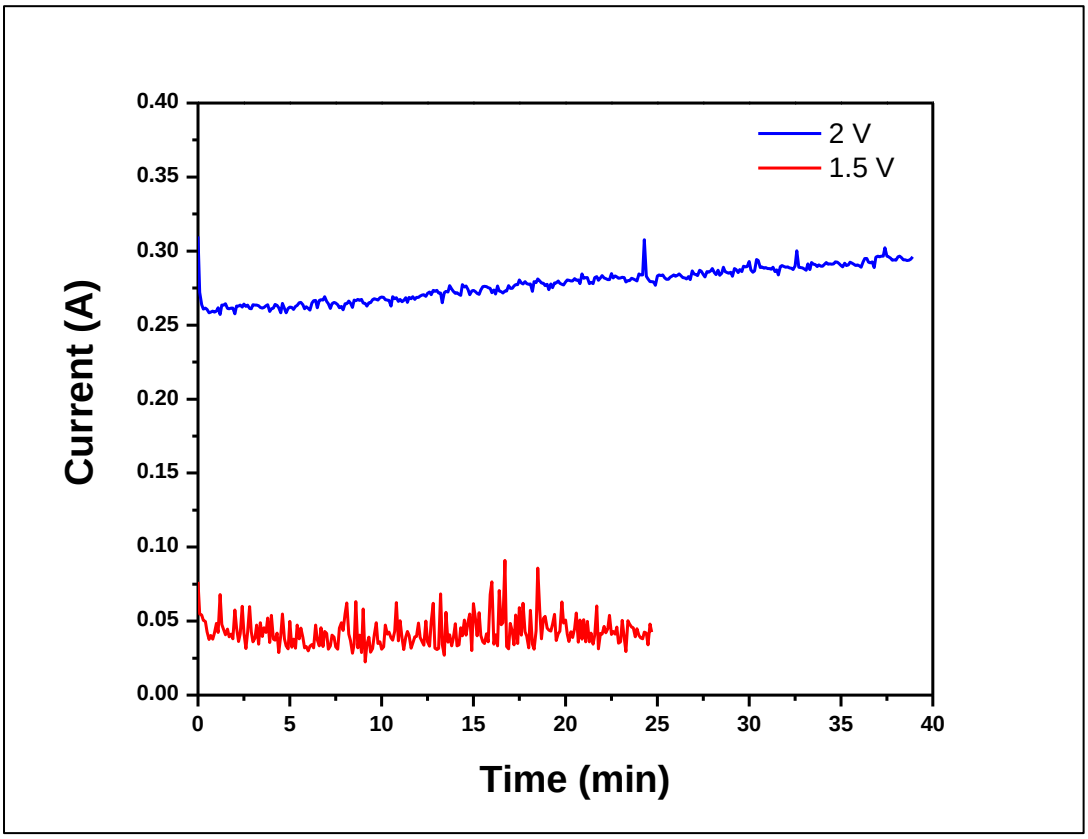

Fig. 4. The current-time plots of electrolysis in molten carbonates at 500 ℃ under two different cell voltages.

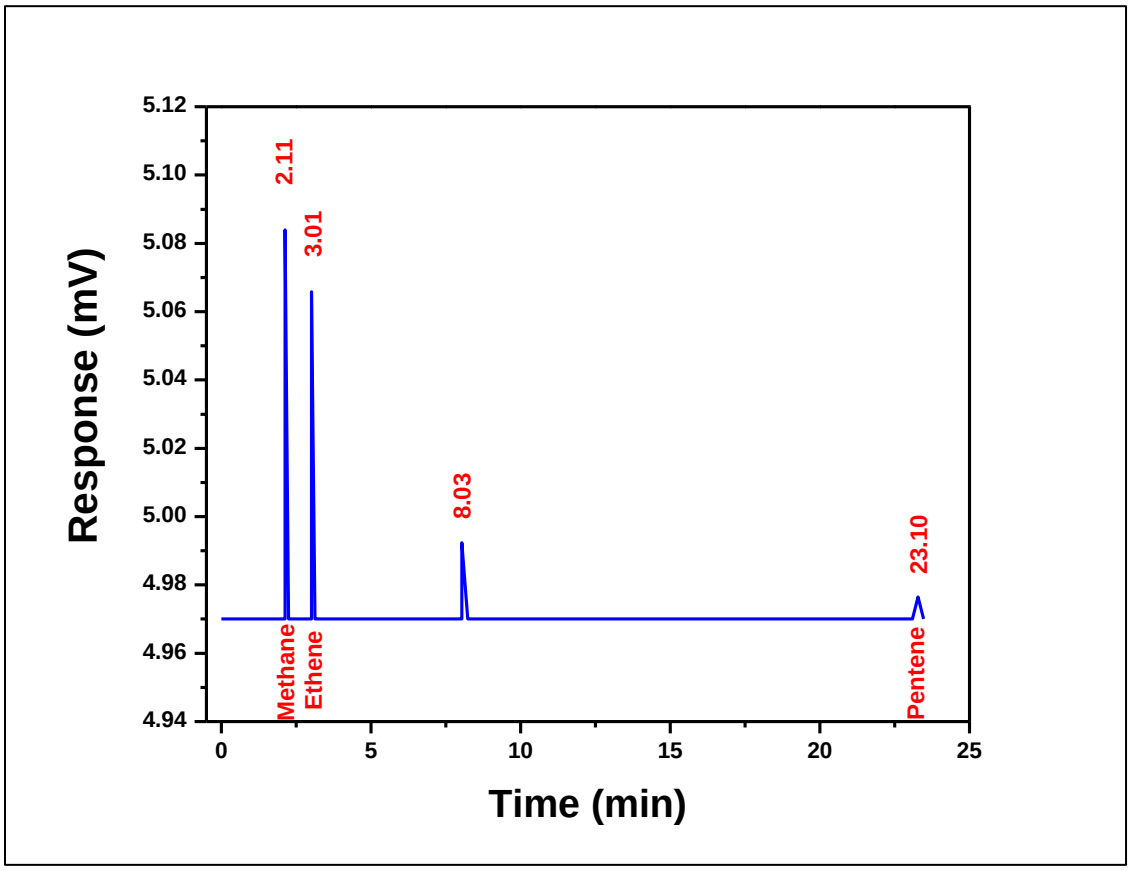

Fig. 5. The FID detector analysis of cathodic gas samples during electrolysis in molten carbonates at 2 V and 500 °C by GC.

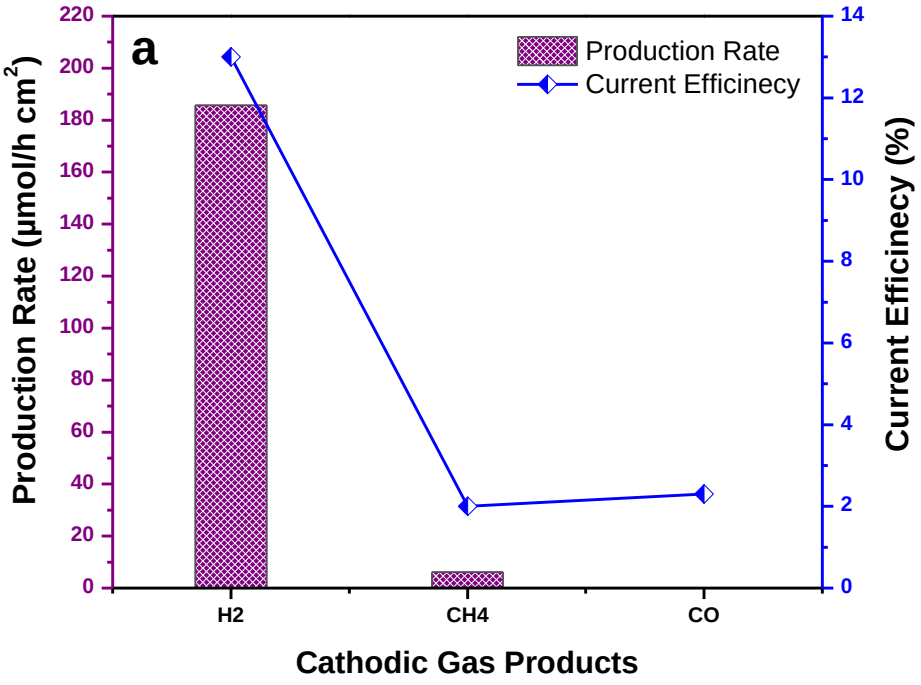

716

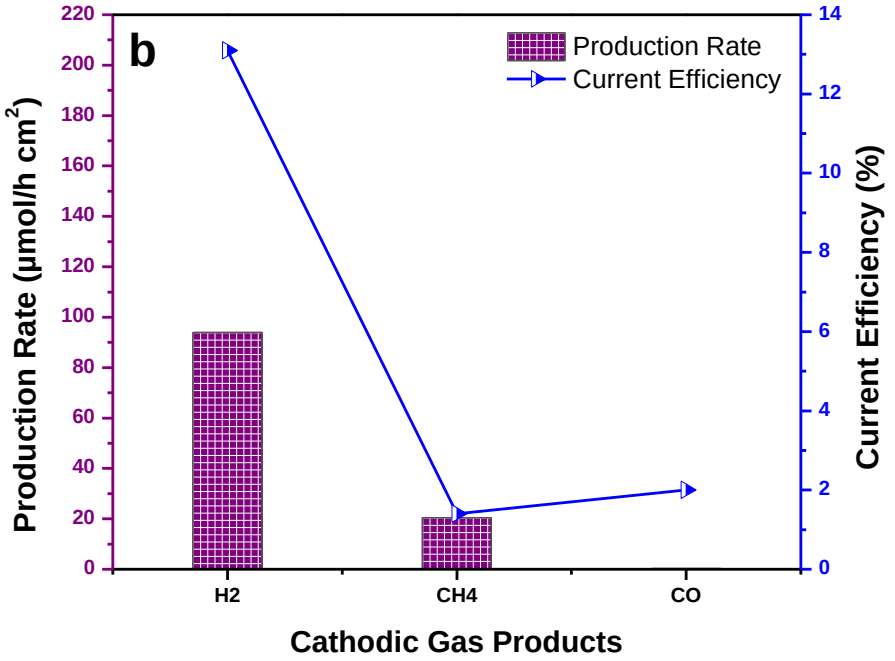

717

718 **Fig. 6.** The cathodic gas products during electrolysis in LiOH-NaOH molten hydroxide at 275 °C
719 under different applied cell voltages; (a) 2 V and (b) 3 V.

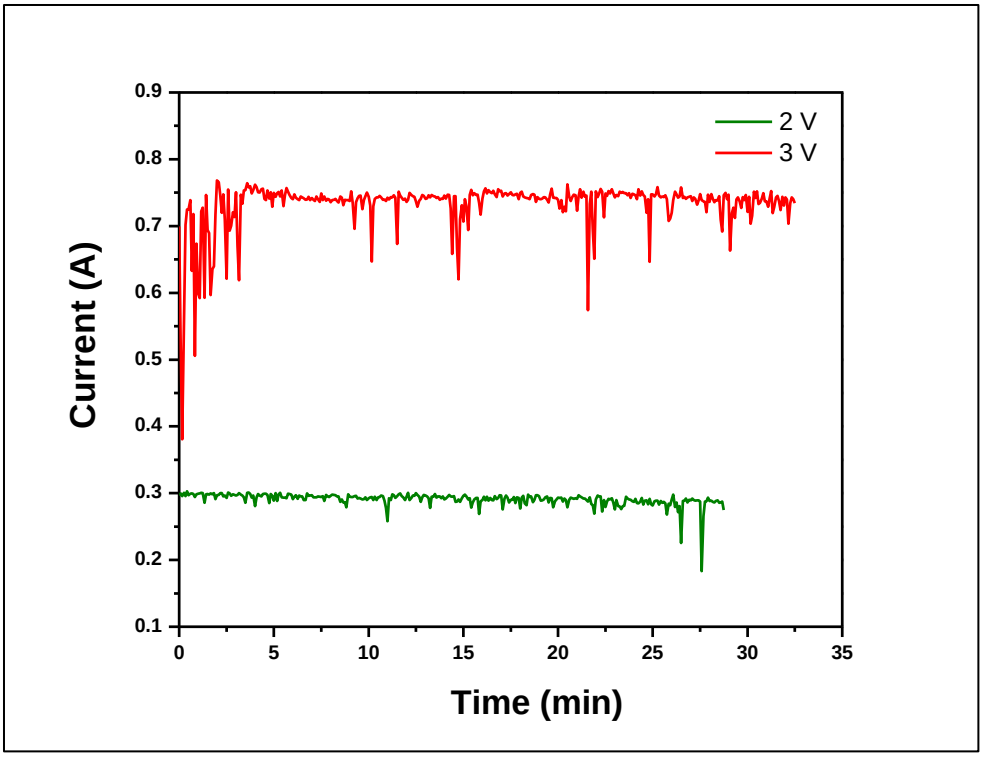

720

721 **Fig. 7.** Current-time plots of electrolysis in LiOH-NaOH (27–73 mol%) molten salt at two different

722 applied voltages.

723

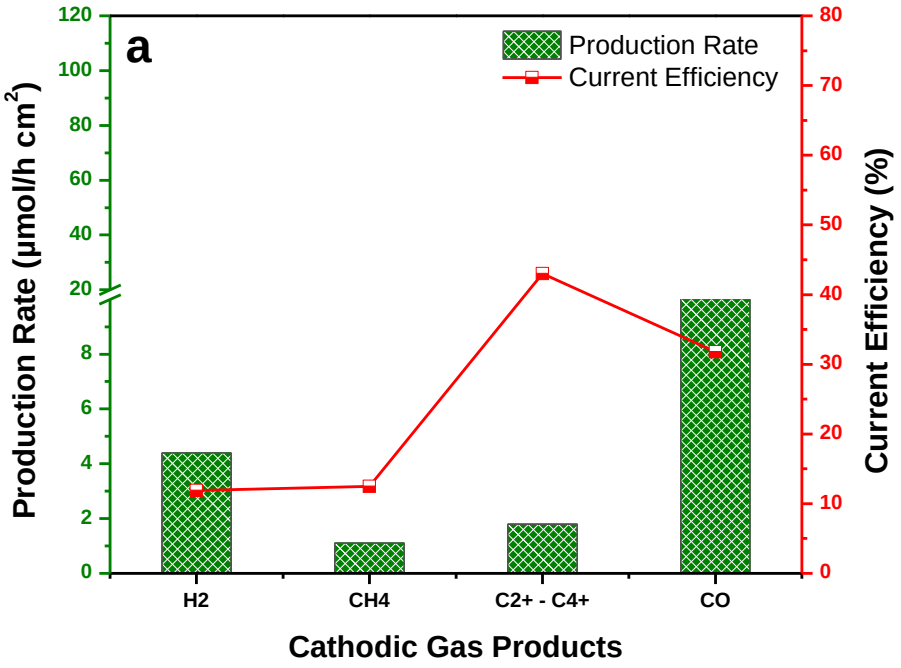

724

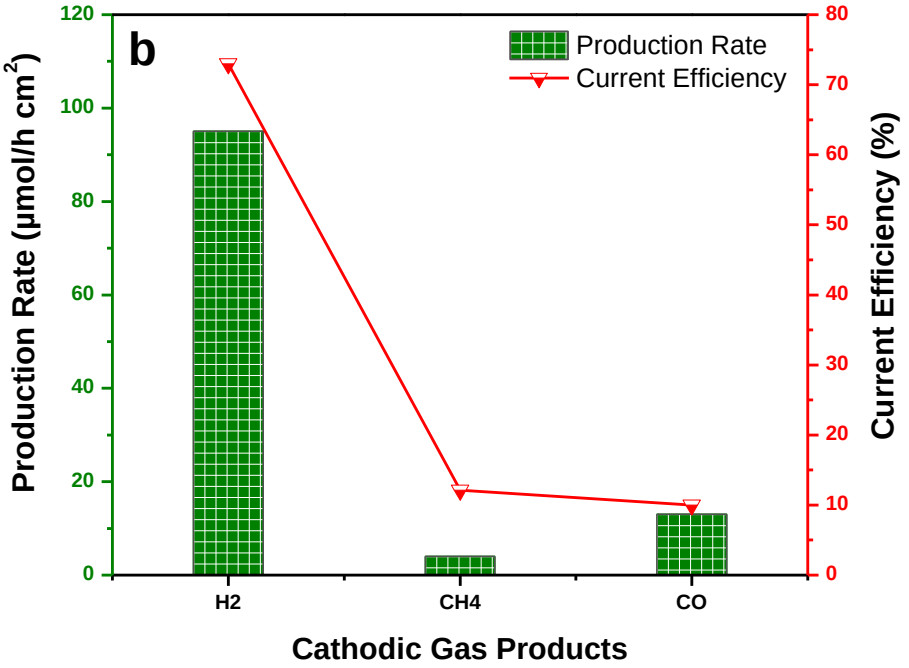

725

726 **Fig. 8**. The GC analysis of cathodic gas products during electrolysis in molten carbonates at 1.5 V
727 and at 425 ℃ with different gas feed compositions of CO_2/H_2O; (a) 15.6, and (b) 9.2.

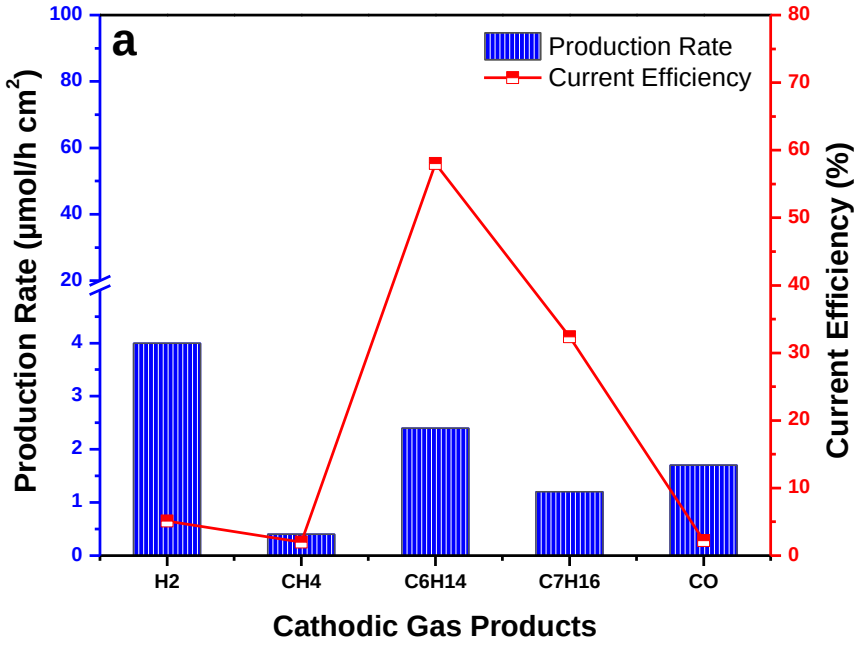

728

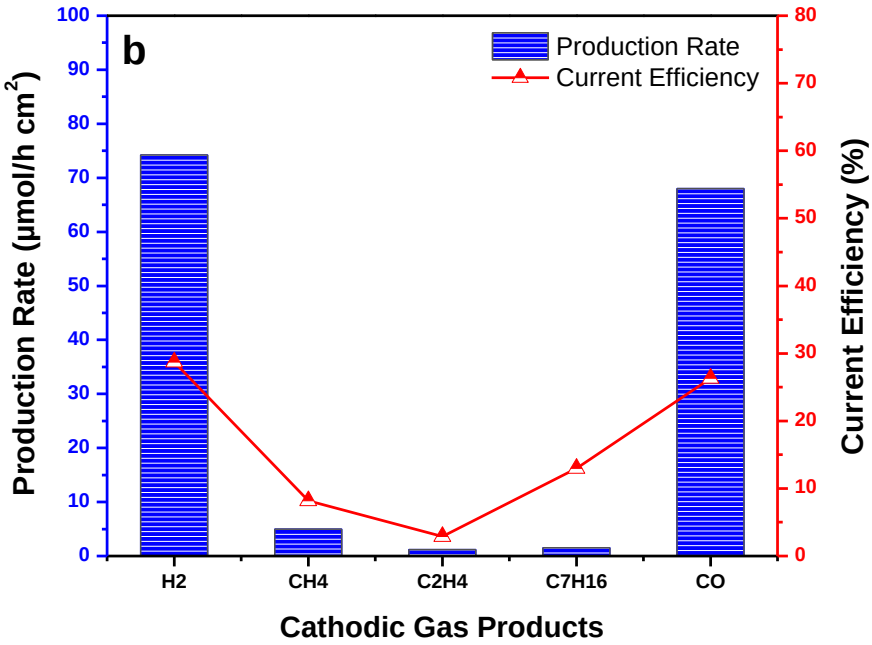

729

730 **Fig. 9**. The GC analysis of cathodic gas products during electrolysis in molten carbonates at 1.5 V
731 and at 500 °C temperature with different gas feed compositions of CO_2/H_2O; (a) 15.6, and (b) 9.2.
732

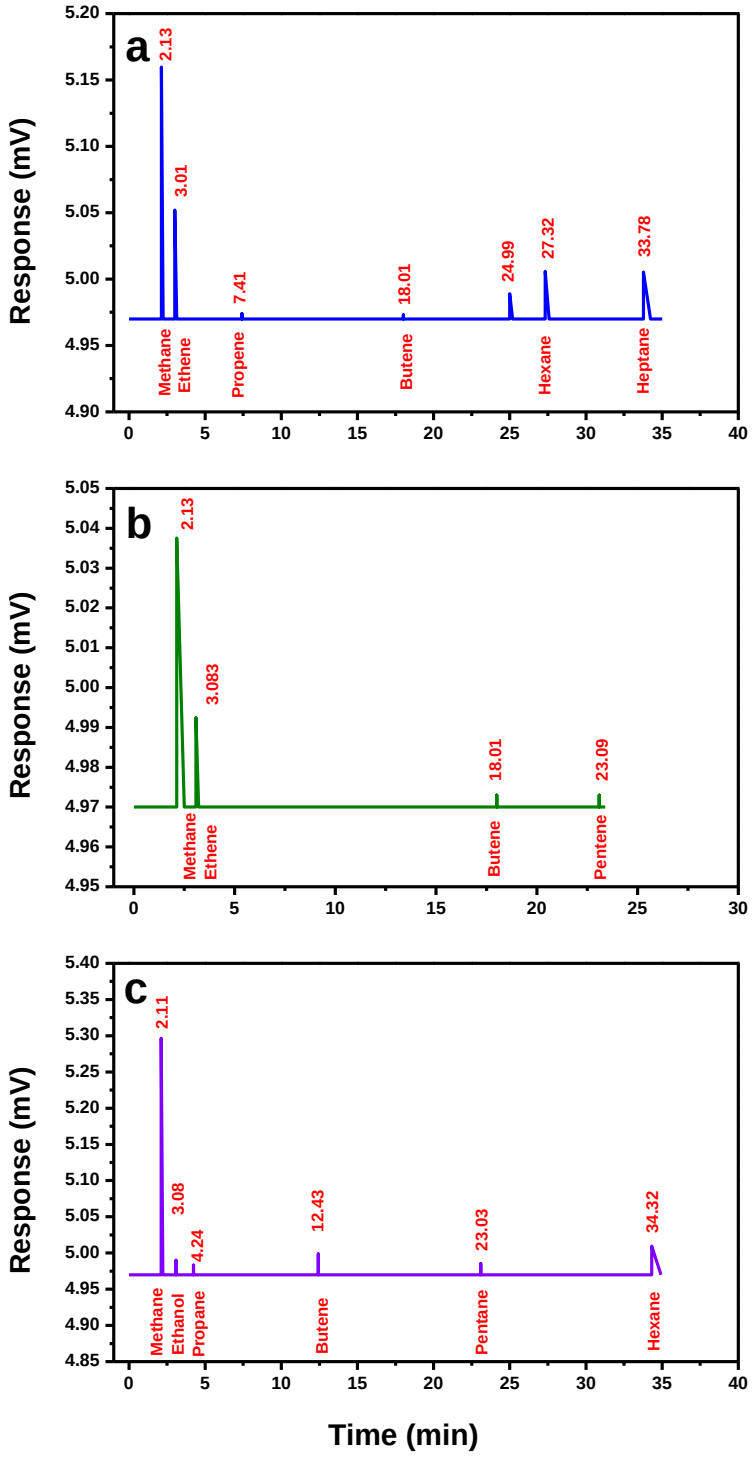

733

734 **Fig. 10.** The FID detector analysis of the cathodic gas samples during electrolysis in molten
735 carbonates at 1.5 V and 500 °C with different CO_2/H_2O ratios; (a) 9.2, (b) 15.6 and (c) 9.00.

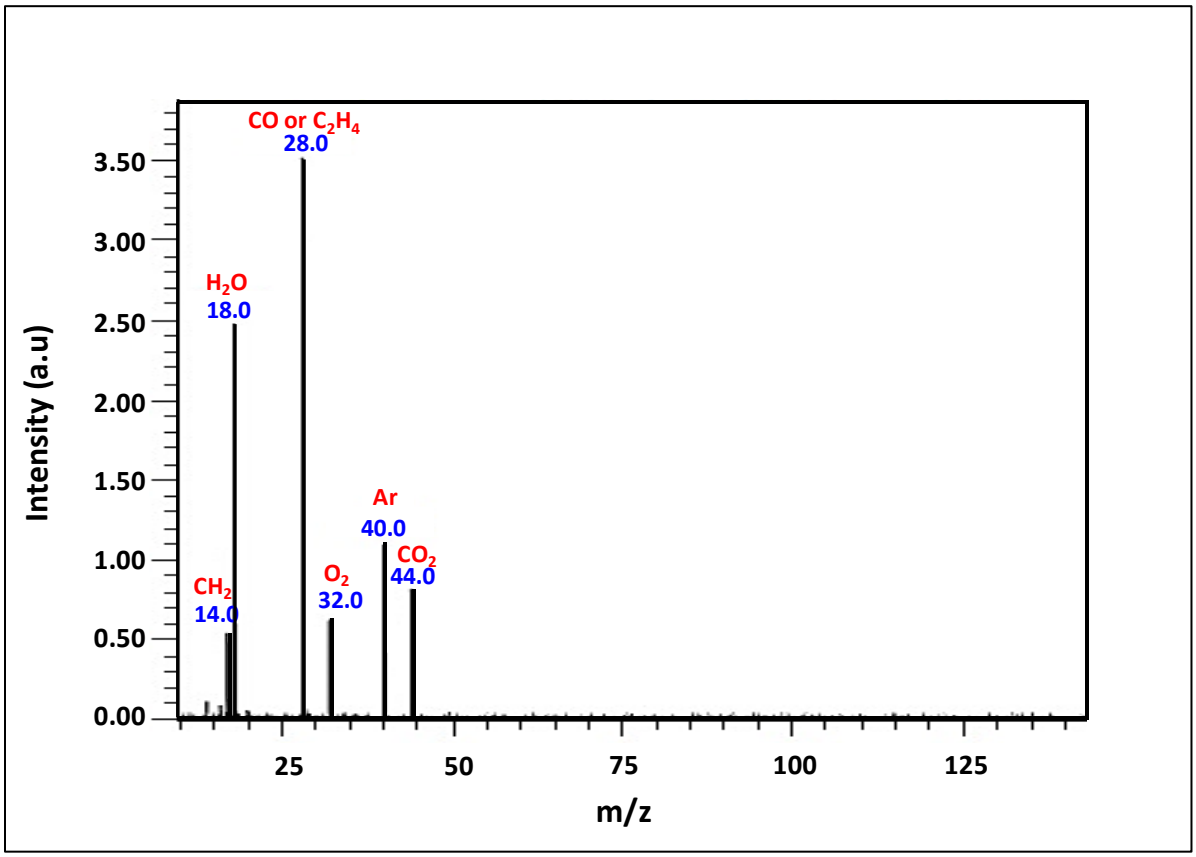

Fig. 11. Mass spectrum of gases between 1–1.04 min retention time in a permanent gas product eluting before the hydrocarbon gas.

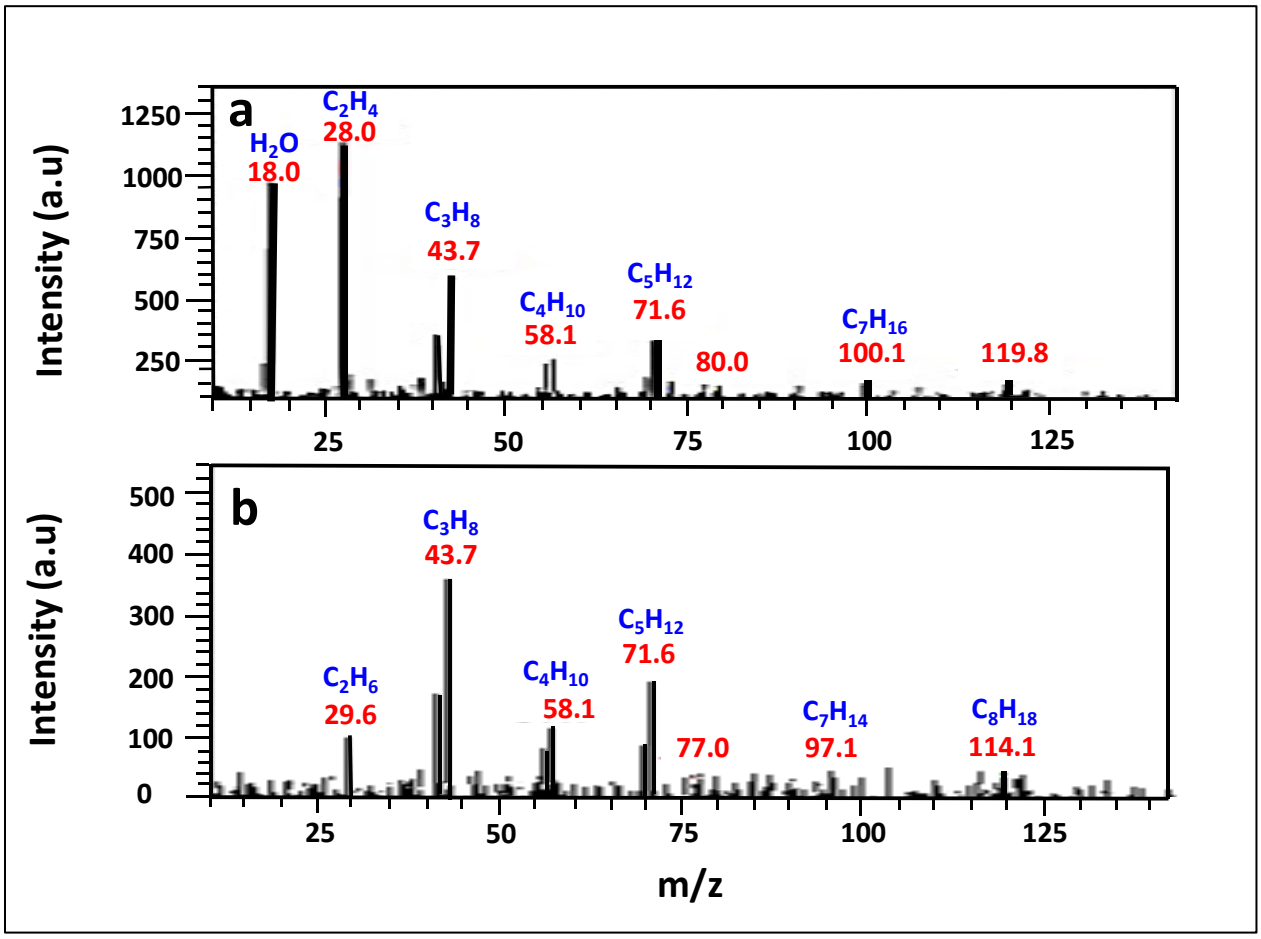

Fig. 12. Mass spectrum of gases eluting at; (a) 1.72 min (before), and (b) 2.9 min retention time (after) subtracting the permanent gases eluting with hydrocarbon product.

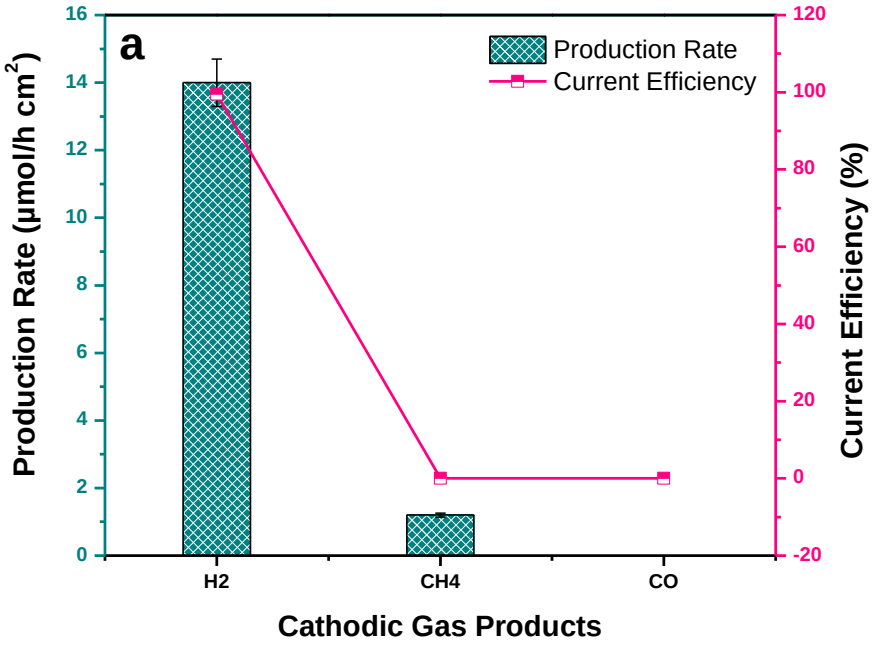

746

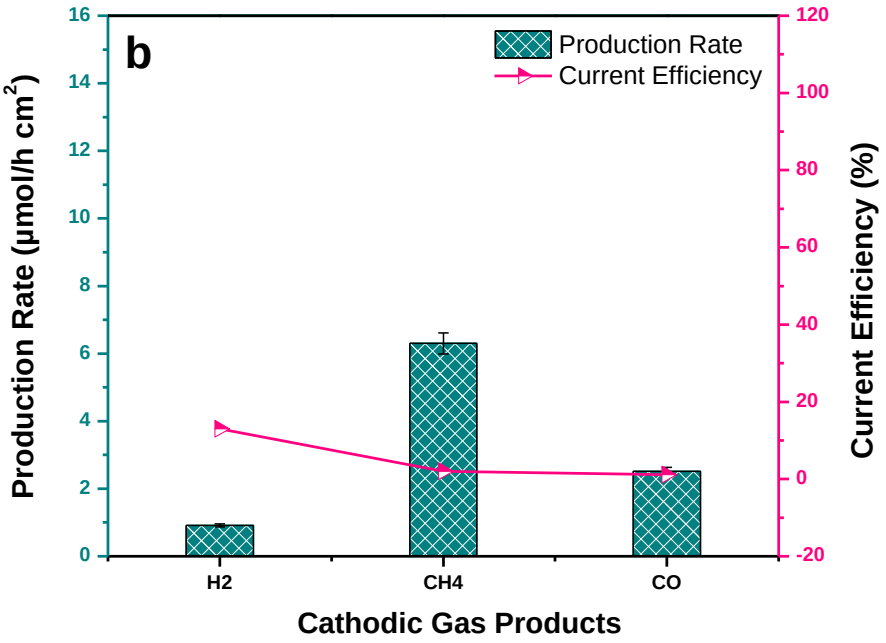

747
748 **Fig. 13.** The GC analysis of cathodic gas products during electrolysis in the molten hydroxides
749 (LiOH-NaOH (27–73 mol%) at 2 V and 275 ℃ with different gas feed composition of CO_2/H_2O;
750 (a) 1 and (b) 5.6.

List of Tables

Table 1. Specifications of the cathodic gas products during electrolysis of molten carbonates at 1.5 V and 425 ℃ by using GC and mass spectrometric analysis.

Product	Gas product composition (vol %)	Production rate (μmol/h cm^2)	Selectivity (%)	Current efficiency (%)	Heating value (J)	Energy consumption (J)
H_2	0.22	4.40	–	11.90	11.40	
CH_4	0.06	1.10	6.80	12.50	10.40	
C_2H_4	0.04	0.80	5.00	13.20	12.00	
C_3H_6	0.03	0.50	3.10	12.70	11.00	
C_4H_8	0.03	0.50	3.10	17.00	14.50	114.20
CO	0.58	11.70	–	31.80	35.30	
CO_2	52.70	–	–	–	–	
H_2O	2.40	–	–	–	–	
Ar	44.00	–	–	–	–	

Table 2. Specifications of the cathodic gas products during electrolysis of molten carbonates at 1.5 V and 500 ℃ using GC and mass spectrometric analysis.

Product	Gas product composition (Vol %)	Uncertainty of gas consumption	Production rate (μmol/h cm^2)	Selectivity (%)	Current efficiency (%)	Heating value (J)	Energy consumption (J)
H_2	0.210	±0.04	4.00	–	5.10	7.30	171.00
CH_4	0.02	±0.016	0.40	7.00	2.00	2.60	
C_6H_{14}	0.12	±0.01	2.40	42.10	58.00	75.00	
C_7H_{16}	0.06	±0.003	1.20	21.00	32.40	43.30	
CO	0.10	± 0.01	1.70	–	2.20	3.70	
CO_2	40.30	–	–	–	–	–	
H_2O	3.10	–	–	–	–	–	
Ar	56.10	–	–	–	–	–	

Table 3. List of ΔrG and ΔrH for the generation of hydrocarbon products from the Fischer-Tropsch reaction (CO_2 or H_2O formation) and partial oxidation of methane at 500 ℃.

Product	Fischer-Tropsch reaction				CH_4 partial oxidation	
	ΔG (KJ/mol)		ΔH (KJ/mol)		ΔG (KJ/mol)	ΔH (KJ/mol)
	CO_2 formed	H_2O formed	CO_2 formed	H_2O formed		
CH_4	-40.29	-29.90	-258.59	-221.37	–	–
C_2H_6	-9.68	11.10	-446.82	-372.37	-134.10	-175.70
C_2H_4	30.28	51.06	-303.79	-229.35	-299.20	-278.80
C_3H_8	14.43	45.59	-525.5	-413.87	-274.70	-241.90
C_3H_6	38.15	69.31	-386.19	-274.53	-456.00	-348.70
C_4H_{10}	28.53	70.08	-684.90	-536.01	-425.30	-388.80
C_4H_8	55.74	97.29	-710.86	-561.97	-603.10	-660.90
C_5H_{12}	54.87	97.31	-1037.57	-609.94	-563.70	-729.00
C_5H_{10}	80.07	132.00	-907.92	-721.82	-743.50	-845.40
C_6H_{14}	72.68	135.00	-1058.63	-835.30	-886.20	-1030.00
C_6H_{12}	102.18	152.06	-1104.99	-696.53	-710.60	-737.50
C_7H_{16}	81.43	154.14	-1219.94	-959.38	-866.60	-886.40
C_7H_{14}	124.29	197.00	-1302.07	-1041.52	-1028.80	-1214.60

Graphical Abstract